Vision at the limits: absolute threshold, visual function, and outcomes in clinical trials

Matthew P. Simunovic ***MB BChir PhD FRANZCO***[1,2*]

John R. Grigg ***MD FRANZCO***[1,2]

Omar A. Mahroo ***MB BChir PhD FRCOphth*** [3-6]

1. Save Sight Institute, University of Sydney, Sydney, AUSTRALIA
2. Sydney Eye Hospital Sydney, AUSTRALIA
3. Moorfields Eye Hospital, London, United Kingdom
4. Institute of Ophthalmology, University College London, United Kingdom
5. Section of Ophthalmology, King's College London, St Thomas' Hospital Campus, London, United Kingdom
6. Physiology, Development and Neuroscience, University of Cambridge, Cambridge, United Kingdom

*To whom all correspondence should be addressed: Save Sight Institute, University of Sydney, 8 Macquarie Street, Sydney NSW 2000, AUSTRALIA E matthew.simunovic@sydney.edu.au T +9382 7111 F +612 9382 7114

Keywords

Photopic vision, scotopic vision, full-field stimulus testing (FST), full-field stimulus threshold, multi-luminance mobility testing (MLMT), psychophysics, electrophysiology, retina

Abstract

The study of individual differences in perception at absolute threshold has a rich history, with much of the seminal work being driven by the need to identify those with superior abilities in times of war. Although the popularity of such testing waned in the latter half of the 20th century, interest in measures of visual function at the absolute limit of vision is increasing, partly in response to emerging treatments for retinal diseases, such as gene therapy and cellular therapies, that demand "new" functional measures to assess treatment outcomes. Conventional clinical, or clinical research, testing approaches generally assess rod sensitivity at or near absolute threshold: however, cone sensitivity is typically assayed in the presence of adapting backgrounds. This asymmetry may artifactually favor the detection of rod abnormalities in patients with outer retinal disease.

The past decade has seen the commercialization of devices capable of assessing absolute threshold and dark adaptation, including specialized perimeters and instruments capable of assessing "full-field sensitivity threshold" that seek to integrate responses over time and space in those with unstable fixation and/or limited visual fields. Finally, there has also been a recent recapitulation of tests that seek to assess the subject's ability to interpret the visual scene at or near absolute threshold. In addition to assessing vision, such tests simultaneously place cognitive and motor demands on patients in line with the activities of daily living they seek to replicate.

We describe the physical and physiological basis of absolute threshold and dark adaptation. Furthermore, we discuss experimental psychophysical and electrophysiological approaches to studying vision at absolute threshold and provide a brief overview of clinical tests of vision at absolute threshold.

Introduction

Although it has perhaps long been overlooked clinically, absolute visual threshold — hereafter assumed to be the minimum light stimulus required to evoke a visual response from a fully dark-adapted receptoral mechanism — has important ecological implications for species possessing the sense of vision. For example, nocturnal animals possess molecular ("stable" photopigments generating little molecular noise; inactivating mutations in genes encoding less sensitive photopigments),[61] physiological (e.g. rod-dominated retinas), and anatomical adaptations (e.g. comparatively large corneas/ entrance pupils[69] and orbits,[67] a *tapetum lucidum*)[19] that are argued to confer small, but significant, biological advantages to absolute visual threshold. Much of the research into visual function at absolute threshold in the first half of the 20th century had been directly or indirectly driven by the engine of war: vision research before and during World War II was partly directed towards identifying and selecting military personnel with superior vision at absolute threshold.[35; 97; 122] These early experiments established a correlation between the absolute threshold of vision, scotopic acuity, and performance at tasks that required interpretation and judgement of complex scenes in normal subjects.[122] Subsequently, interest in this aspect of vision saw something of a decline, despite the fact that many retinal diseases appear to preferentially affect photoreceptor function at absolute threshold.[57; 116; 117] More recently, however, there has been a resurgence in the level of interest in absolute threshold as the result of emerging treatments for retinal disease, including gene therapy, stem cell therapy and electronic retinal prostheses.[33; 64; 104; 105; 112] This, in turn, has led to the reintroduction of tests designed to determine absolute threshold and practical tasks of vision conducted at, or near, absolute threshold.

Here, we provide a brief overview of the machinery of vision at the retinal level and describe the physical and physiological basis of absolute threshold and dark adaptation. Next, we discuss briefly experimental psychophysical and electrophysiological approaches to studying vision at absolute threshold and conclude by discussing clinical tests of vision at absolute threshold.

1. THE MACHINERY OF VISION

The human visual system can operate over a vast range of luminance levels, spanning at least 10 log units.[118] The (entrance) pupil of the eye can only adjust itself over a range of approximately 2 to 8 mm in diameter, giving a little over 1 log unit of control over retinal illuminance. In part, the wide range of functioning of the human visual system is possible because the retinal receptor system is duplex in nature: the two morphologically distinct photoreceptors operate over a different range of luminance levels: the rods being used at lower illumination levels (scotopic levels), while the cones are used when illumination levels are higher (photopic levels).[115] An additional class of photoreceptors has

more recently been identified: the intrinsically photosensitive retinal ganglion cells (ipRGCs). These were initially thought to be involved exclusively in regulating non-image forming vision via non-cortical pathways – mainly the pupillary light reflex[1; 29; 50] and diurnal entrainment; however, emerging evidence supports a possible contribution to cortically-mediated visual processing.[25; 29; 129; 146]

In common with other mammals, rod photoreceptors comprise the bulk of the photoreceptor population in humans — approximately 120 million in total — despite being a relatively recent addition in evolutionary terms. The cone photoreceptor population is roughly 5% of that of the rods, at about 6 million per eye.[2; 87] The cones have their peak density at the fovea (300,000 cells.mm^{-2}) and their density declines sharply with increasing eccentricity, except for a steep increase at the ora serrata.[2] The rods, by contrast, are absent from the most central retina, but otherwise have a comparatively constant density that peaks at about 160,000-190,000 cells.mm^{-3} at 20-30° eccenticity.[2] The rods and cones differ in several important respects, and many of these differences combine to determine each system's sensitivity at absolute threshold. Both classes of photopigment absorb light via a photopigment that consists of a heptahelical protein, or opsin, covalently bound to 11-cis-retinal, which is in turn derived from vitamin A.[81] Opsins are members of a superfamily of G-protein-coupled receptor molecules, and absorption of a light quantum leads to isomerization (so-called "photoisomerization") which in turn activates an amplifying cascade of reactions ultimately leading to the closure of cation channels in the photoreceptor outer segment membrane. This leads to hyperpolarization and a decrease in the release of neurotransmitter (glutamate) into the synaptic cleft.[144; 145]

The signal is taken up again by the second-order neurons – the bipolar cells – of which there are a dozen physiologically and/or morphologically distinct types.[87] These may receive input from either rods[141] or cones. Further, cone bipolar cells are specialized to receive input from different photoreceptor classes.[87] At the fovea a single cone photoreceptor may uniquely provide input to a single bipolar cell. As the name coincidentally implies, bipolar cells convert the unipolar response of photoreceptors into a bipolar signal by either depolarizing (ON -bipolar cells) or hyperpolarizing (OFF-bipolar cells) in response to light. Furthermore, their responses are "tuned" through lateral interactions mediated by horizontal cells, and they provide inputs into the tertiary neurons of the retina: the retinal ganglion cells (RGCs).[87] Rod bipolar cells (which are exclusively ON-bipolar cells) do not synapse directly to ganglion cells, but rather make a connection via the All amacrine cell[142] to the ON- and OFF- cone bipolar cells which, in turn, synapse with ganglion cells. Thus the cone system piggybacks the rod system.[138] In the central retina, each rod spherule contacts two rod bipolar cells,

which in turn contact approximately five AII cells. Simultaneously, there is neural convergence in the rod pathway; around 500 rods converge on one AII cell. The rods are apparently represented in both the magno- and parvocellular systems. Scotopic acuity is believed to be too high to be supported by the magno system alone.[80] In turn, the RGCs are highly specialized, with separate populations carrying information in parallel.[87] For example, there are at least 4 types of distinct RGC specialized for processing signals received from the S-cones, though there are no rod-specific RGCs.[87; 127] It will be noted that a significant amount of processing of the incoming light signal is performed in the retina through complex cellular networks that act in parallel.[143]

The rods demonstrate greater convergence onto retinal ganglion cells than the cones, an unsurprising fact given the total population of rods (120 million), cones (6 million) and RGCs (1.125 million).[36] Rods derive a greater sensitivity than cones through the cumulative effects of a variety of adaptations. The rod photopigment, rhodopsin, is believed to be fundamentally more stable (i.e. less prone to spontaneous "quantal-like" events) than the cone photopigments. This was initially hypothesized to be a function of its wavelength of peak sensitivity (λ_{max} = 496nm; see Figure 1)[37] by Barlow,[12] but has also been proposed to reflect other molecular factors which alter thermal stability.[91] In addition to being less "noisy" than the cone photopigments, rhodopsin also appears to be more efficient in its interaction with the effectors of the phototransduction cascade.[58] Additional factors also help improve the rod's sensitivity at the cellular level, including outer segment morphology.[58] The kinetics of rod activation are such that they integrate the incoming light signal over a longer time course (at the expense of temporal resolution).[58] The aforementioned convergence onto second- and third-order retinal neurons also integrates rod responses over space,[39] which again affords overall improvements in sensitivity at the expense of spatial resolution.

2. SIGNAL VS NOISE & ADAPTATION TO ABSOLUTE THRESHOLD

The task of the visual system is to detect a light signal incident on the retina. This "signal" is not detected in isolation, but rather, it is detected in the presence of "noise". This noise may be inherent in the signal itself or present at the receptoral or post-receptoral level.

a. *Quantal fluctuations/signal noise*

Hecht, Schlaer, and Pirenne[52] were the first to apply quantum theory to the analysis of signal detection by the visual system. Previously, it had been assumed "that the stimulus is constant and the organism variable".[52] They demonstrated, however, that there is inherent variability in the stimulus itself.

If we consider the case of a shutter opening and closing at regular intervals to present a stimulus of fixed size, duration and radiance, the number of quanta delivered at each "opening" is not constant. Instead, the number of quanta follows a Poisson distribution. If the eye were a perfect detector, then absolute sensitivity would depend only upon this quantal variation, which has been termed "quantum noise".[86]

b. Dark noise

Barlow demonstrated that quantum noise could not account for psychophysical estimates of absolute sensitivity; he proposed that there must also be a source of noise within the observer.[11] The amount of Poisson noise that must be delivered to an ideal detector to degrade its performance to the level of a human observer is termed the "dark noise".[86] Such "noise" can be attributed to two distinct mechanisms:[118]

i. Receptoral noise: This form of noise is generated in the rod itself and may be the result of spontaneous closing and openings of cGMP channels in the rod outer segment[75] from fluctuations in the concentrations or lifetimes of the biochemical intermediates of the phototransduction cascade (including the lifetime of activated rhodopsin), from reverse reactions in the inactivation of isomerized rhodopsin following intense bleaches, or from thermal isomerizations. In total darkness, rods display quantal events similar to those observed at low light levels. The phenomenon was first observed in the toad rod,[16] and then in the primate rod.[17] The rate of spontaneous quantal events in simian rods has been used to account for dark noise in human observers.[76] In the toad rod, it is estimated that spontaneous isomerization occurs approximately every 50 seconds or so. Because the number of rhodopsin molecules per rod is known, one may calculate the spontaneous isomerization rate of one rhodopsin molecule. There are approximately 2 $x10^9$ rhodopsin molecules in one toad rod. If we multiply this number by the total rate of spontaneous isomerizations, we find that one rhodopsin molecule will display a spontaneous isomerization once every 10^{11} seconds (about 3200 years). The rate of spontaneous quantal events arising in total darkness from the rods of *Macaca fascicularis* is 0.0063 per second (once every 2min 39sec at 37°C).[17] These spontaneous events are thought to be primarily the result of thermal isomerizations of rhodopsin molecules.[76] Receptoral sources of noise may be additive in nature (i.e. the noise is continuously present and/or independent of the strength of the signal) or multiplicative (i.e. proportional to the magnitude of the signal).[118]

ii. Neural noise. It can be shown psychophysically that the total internal noise is equivalent to a rate of up to 0.04 isomerizations per second (i.e. as high as once every 25 sec).[86] If the rate of spontaneous isomerizations for the isolated monkey rod can be used to approximate the rate occurring in human

rods in vivo, then it becomes apparent that not all of the noise that limits absolute threshold arises from the photoreceptors.[86] It has previously been estimated that around half of the total internal noise is due to neural noise.[14] Such neural noise may result from the spontaneous release of neurotransmitter from synaptic terminals, fluctuations in the threshold for the initiation of nerve impulses and the threshold criterion of the subject.[118] Evidence gained from power spectral analysis of the discharge of ganglion cells in the cat suggests that irregularities remain roughly constant when the discharge rate is raised or lowered by visual stimulation (and thus, the noise is assumed to be largely additive rather than multiplicative).[102]

c. *The effects of pathology on the signal to noise ratio*

Derangements of normal physiology can be conceptualized as altering the strength of the incoming signal, the level of noise, or both. For example, decreases in the quantal efficiency of the photoreceptors, e.g. through defects arising from reductions in the optical density of the photopigment in the outer segments or alterations to the opsin itself,[8] are anticipated to result in a decreased neural signal; however, specific mutations – particularly dominant "gain of function" mutations – may result in constitutively active components of the phototransduction cascade.[44] This may effectively increase inherent noise (while also decreasing signal). Alterations in the signal to noise ratio at the level of the photoreceptors and at the post-receptoral level have the effect of elevating absolute threshold; however, analysis of threshold versus intensity functions suggests that they have different effects once light adaptation commences.[57; 116; 117; 126] Receptoral pathology is hypothesized to result in a so-called "filter effect". This translates threshold versus intensity functions upwards and rightwards (See Figure 2) and has been termed $d_{1/2}$ mechanism loss.[57] Post-receptoral pathology, however, is theorized to result in upwards translation only; this is known as d_3 mechanism loss.[57] These observations have important implications for clinical testing and underscore the power of assessing photoreceptor mechanisms at absolute threshold.[126] In particular, assessment at absolute threshold is predicted to detect alterations from both pathology resulting in $d_{1/2}$ mechanism loss, as well as d_3 mechanism loss.[65; 126] Probing sensitivity at higher background intensities — for example where Weber-like behavior is demonstrated — may fail to elucidate $d_{1/2}$ mechanism loss (but not d_3 mechanism loss; see Figure 2).[126] The assessment of vision at absolute threshold is not without its costs. In particular, sensitivity estimates will be vulnerable to pre-receptoral effects, including pupil size and pre-photoreceptor absorption by the ocular pigments (leaving aside long-term retinal/neural adaptation to the latter).[123; 124; 126]

d. *Adaptation to absolute threshold*

Dark adaptation can be considered as the recovery of visual sensitivity following adaptation to a background illuminant that bleaches[l] a fraction of the photopigment in the photoreceptors. This process is relatively slow: it may take up to 40 minutes for dark-adapted sensitivity to be regained following an intense bleach.[100]

In the isolated retina, there is an association between the bleaching of rhodopsin and exposure to light.[110] It is unsurprising, therefore, that a link has been sought between the time course of recovery of visual sensitivity following a bleach and the regeneration of rhodopsin. Early experimental evidence demonstrated that the time course of rhodopsin regeneration in the frog retina roughly corresponded to that of dark adaptation.[100] With the invention of fundus reflectometry, it became possible to study the time course of rhodopsin regeneration objectively in humans, *in vivo*. Using this technique, Campbell and Rushton[28] demonstrated that the absorption properties of the dark-adapted eye closely approximated that of rhodopsin. This finding was later confirmed by Alpern and Pugh,[7] who compared psychophysically determined dark-adapted spectral sensitivity to the action spectrum of lights producing a 10% bleach.

The time course of regeneration of the visual pigments was described as an exponential function by Rushton:[107; 108]

$$B = B_0 * e^{\frac{-t}{T}}$$

Where B is the proportion of pigment that remains bleached, B_0 is the proportion of pigment bleached initially, t is time, and T is the time constant of recovery. Rushton[107; 108] suggested that the log sensitivity recovery, like that of the pigment regeneration rates, followed an exponential time course with similar dynamics. This was supported by electrophysiological research conducted by Dowling in the rat.[42] Threshold elevation was described according to an equation now known as the Dowling-Rushton relation:

$$\frac{\Delta I}{\Delta I_0} = 10^{aB}$$

Where ΔI is threshold elevation and ΔI_0 is absolute threshold and a is equal to 12.[6]

[l] Early researchers investigating the reaction to light of "Sehpurpur" (i.e. rhodopsin) noted that it turns from magenta to orange then yellow, and ultimately to white. This process was therefore called "bleaching". The term "bleach" has come to be synonymous with the activation and subsequent depletion of rhodopsin by light.

Rushton's model can still be viewed as an empirical description that provides no underlying mechanistic explanation.[100] It still appears in texts on ocular physiology and is widely employed in the clinical literature;[40; 122] nevertheless, there are some problems with it. With very small bleaches, the model underestimates the amount of threshold elevation (by as much as 1 log unit).[76] With large bleaches at early timepoints, the estimation is even worse.[76] Rushton's model also requires a pooling of the rod signals over a large area of the retina at a site proximal to the receptors.[76] Support of this theory was found when bleaching was performed using either stripes or dots.[109; 110] However, subsequent experiments with striped bleaching lights demonstrated that sensitivity in regions where dark bars had been imaged was not reduced to the same extent as in regions where the bleaching bars were imaged.[13] The other problem is with the time course of recovery. Pugh investigated the value of *T* with different bleach intensities and found that it was not constant, but rather varied with B_0.[98] Over substantial periods, Lamb suggests the recovery in rod sensitivity following a bleach can be described well by straight lines.[76; 78]

Using the psychophysical data of Pugh,[98] Lamb[74] demonstrated in 1981 that recovery from a wide range of bleaches has three components, possibly corresponding to the exponential decay of three intermediate substances within the rod photoreceptors (named S1, S2 and S3, with time constants of approximately 5 s, 100 s and 7 min respectively). A striking feature of the S2 component for bleaches of more than 20% was that the time taken for recovery to a threshold criterion increased linearly with bleach level. This indicated that the decay of this substance appeared to be "rate-limited", such that the initial kinetics were linear and not exponential with time.

Mahroo and Lamb[84] later explored photopigment regeneration in cones indirectly by tracking recovery of the dim-flash cone ERG a-wave following bleaching exposures and found that regeneration following a range of bleaches appeared to proceed with the same common initial linear rate. This was consistent with a rate-limited process rather than the first order kinetics previously assumed by Rushton and others. Their model also provided a better fit to pigment regeneration data measured by retinal densitometry. Figure 3 shows the difference between the two models. Lamb and Pugh[77] showed that such rate-limited kinetics also provided a good explanation for rod-mediated recoveries, consistent with a range of densitometric, electrophysiological, and psychophysical data (this has been termed the Mahroo-Lamb-Pugh, or MLP, model of pigment regeneration kinetics). They identified the S2 component of recovery as being consistent with the removal of free opsin. In rods, free opsin can activate the phototransduction cascade,[34] thus desensitizing (effectively light-adapting) the scotopic visual system, explaining the profound psychophysical threshold elevation following

bleaching exposures. As free opsin is "removed" by the delivery of 11-cis retinal to the photoreceptor outer segments (forming rhodopsin), sensitivity recovers. Such rate-limited kinetics in both rods and cones can emerge from modelling diffusion of 11-cis retinal into the outer segments from a pool of retinoid through a resistive barrier. The pool was presumed to be in the RPE, although cones also have access to a Müller-cell mediated pathway.[88] Mahroo and Lamb[85] later found that following extremely intense bleaches, the rate of cone-mediated recovery as measured electrophysiologically slows further (though the initial recovery is still clearly linear, rather than exponential), possibly indicating depletion of the retinoid pool.

Lamb and colleagues in 2015[79] presented data to show that the rate-limited kinetics described above can also emerge from modelling of an enzymatic, rather than a resistive, rate limit. They provided arguments favoring the former as the basis of the kinetics seen in human rod and cone photopigment regeneration, and hence dark adaptation. Interestingly, electrophysiological recordings following intense bleaches suggest that there may be a readily available pool of cone opsin and one that is regenerated more slowly.[68; 85] It is known that there is a Müller cell-mediated pathway of photopigment regeneration (in addition to the slower canonical RPE-mediated visual cycle) thought to be accessible exclusively by the cones:[88] such data perhaps reflect the depletion of a "pool" made available via this faster pathway.

Melanopsin regeneration kinetics are proposed to follow an exponential time course with time-constants of regeneration intermediate between those of rhodopsin and the cone pigments.[93] Although melanopsin can be autonomously regenerated within ipRGCs,[128] regeneration under normal circumstances appears to be supported by both the RPE and the Müller cells.[147]

3. PSYCHOPHYSICAL ESTIMATES OF ABSOLUTE THRESHOLD

Hecht, Schlaer, and Pirenne demonstrated in a landmark experiment that rods can detect the absorption of a single photon,[52] something that took decades to be confirmed independently via single cell electrophysiology.[15; 99] In their classic experiment, which followed complete adaptation to darkness (40 minutes in a dark room), sensitivity was probed with brief (1ms) cyan (510nm) stimuli presented at 20° in the nasal field of vision. The stimuli were small – 10 min of arc – smaller than the limits of rod spatial summation/convergence onto a single RGC. It was estimated that the eye could detect 54 to 148 quanta incident on the cornea. Hecht and colleagues estimated that light loss from interface reflections (principally the cornea; estimated to be 4%), absorption by the ocular media (estimated as a further 50%), and the retina itself (estimated as an additional 80%) significantly attenuated the signal. By their calculations, only between 9 and 10% will reach the photoreceptors

(estimated as 5-14 quanta). A 10 min arc stimulus was predicted to fall on an area containing 500 rods. The probability of any one rod receiving a signal of two quanta was estimated at 4%. These observations led them to conclude that single quantal absorption by 5-14 rods occurs at absolute threshold under these conditions.[52] More recently, it has been demonstrated that the human visual system is even more sensitive than initially supposed by Hecht and colleagues: Tinsely and coworkers employed a quantum light source to demonstrate psychophysically that human rods are capable of detecting a single quantum incident at the cornea with greater than chance probability.[136]

The absolute threshold of the cone mechanisms can be assessed psychophysically via manipulations of the target wavelength (long wavelength targets favor detection by the M+L-cone mechanism),[125] adapting conditions (dim adapting backgrounds may be sufficient to adapt the rod mechanism, but insufficient to significantly elevate the threshold of the cone mechanisms from absolute values; differences in bleach recovery times may also be used to assess cone absolute threshold prior to the cone-rod break),[126; 133] stimulus size, duration (brief/flickering, small stimuli favor detection by the M+L-cone mechanism)[73] and stimulus location (foveal presentation favors the M+L cone mechanism).[73]

Absolute threshold is affected by stimulus parameters, including the size, duration and spectral composition of the stimulus.[55; 119; 125; 140] It will also be noted that, while testing under conditions of absolute threshold has the advantage of uncovering losses in sensitivity not revealed when the visual system exhibits Weber-like behavior (see above),[126] it also introduces the possibility of variations in sensitivity introduced through non-retinal/pre-receptoral variations, including the entrance pupil size of the eye and filtering by the ocular media.[126]

It is important to note that the conventional way of determining the minimum light stimulus required to detect a target is arguably ethologically unsound. Predators do not emit light, and might absorb more light than their surrounds, so in dim environments may be even darker than the surround. What is presumably of adaptive advantage is to detect, in a very dimly lit environment, an object that is even darker than its surroundings, i.e. the minimum decrement detectable at some very low ambient intensity. Such a threshold involves more variables and is understandably more complicated; however, it might arguably be more representative of the natural situation.

4. ELECTROPHYSIOLOGICAL ESTIMATES OF ABSOLUTE THRESHOLD

The conventional approach in the clinical electrophysiology of vision differs from psychophysics: instead of estimating the threshold for a visual response, the amplitude and time course of electrical responses generated from the retinal circuitry for pre-defined stimuli are assessed. Early attempts at

estimating the threshold of vision via electroretinography (ERG) were marred by the inherent noise in obtaining recordings, and thresholds for single stimuli were approximately 1.5 log units above the psychophysical threshold for rods under dark-adapted conditions.[46] The application of signal averaging in the 1960s improved this difference to 0.6 log units, which allowed for the recognition and recording of a small corneal negative wave.[46] This wave was reported to be obscured by the b-wave at around 3.3 log units above the absolute threshold of vision.[46] Recording of scotopic threshold ERGs remains a specialized technique that is not part of the standard clinical armamentarium, and measurements of this kind have come to be known as the "scotopic threshold response" (STR), a term first applied to electroretinograms from animals[120] and later to the human ERG.[121] The original supposition was that the STR represented a form of rod a-wave;[46] however, it was subsequently determined through comparative studies that it is likely to arise from post-receptoral cells.[120; 121]

The isolation of cone-driven from rod-driven responses is challenging and most often involves light adaptation and/or manipulation of the spectral composition of the stimulus or its temporal properties. The standard clinical method of recording cone-driven responses is by delivering stimuli in the presence of a white background (30 photopic cd m^{-2} through a pharmacologically dilated pupil) that preferentially adapts the rods; however, this background also significantly light adapts the cones, and so the dark-adapted cone response cannot be evaluated. Nevertheless in some conditions, cone function may be selectively impaired in the light-adapted state. Dim red flashes delivered in the dark-adapted state are sometimes used to assess the dark-adapted cone-driven responses: these give rise to a shorter latency "x-wave" arising from cone-driven bipolar cells that precedes the larger b-wave arising from rod-driven bipolar cells. Other techniques include the delivery of stimuli in the presence of a dim blue background of sufficient scotopic luminance to desensitize the rods, but of low photopic luminous efficacy, such that the cones are minimally adapted, or soon (e.g. 300 ms) after extinction of such a background, or closely (approximately 1 s) following a prior bright flash at a time point at which the cones, but not the rods, have recovered sensitivity.[23; 24; 94; 103; 139]

It is important to note that specialized protocols for determining ERG thresholds against backgrounds of increasing intensities reveal that the same issues described above for psychophysical estimates also apply to ERGs.[116] That is, $d_{1/2}$ mechanism loss is believed to result in upwards and rightwards shifts in the ERG threshold versus background intensity function, whilst d_3 mechanism loss results in an upwards shift. This means that the most sensitive means of probing loss due to outer retinal pathology may theoretically be under conditions close to absolute threshold.

5. CLINICAL ASSESSMENT OF VISION AT ABSOLUTE THRESHOLD

a. Dark Adaptation

A typical dark adaptation curve is seen in Figure 4. Following the cessation of a bleach, the visual system's sensitivity recovers rapidly for the first minute or so and then reaches a plateau. In this portion of the curve, threshold is determined by the cone photoreceptors. Previous studies have modelled kinetics of cone system dark adaptation following various bleaches.[95] After several minutes the visual system undergoes a second drastic recovery in sensitivity. In this portion of the curve, it is the rod photoreceptors that govern threshold. Rod mediated thresholds can be divided into two components – the so-called S_2 and S_3 phases (see Figure 3).[78] The transition between the cone and rod portions of the dark adaptation curve is often termed the cone-rod break. The experimenter can vary the time of the cone-rod break simply by altering certain features of the stimulus: for example, if one were to use a long wavelength stimulus, this would favor detection by the cone system, as the ratio of the luminous efficiencies for the $V\lambda$ (i.e. M+L-cone mechanism) and $V'\lambda$ (i.e. rod) functions will be maximal for long wavelengths; hence the break occurs later in the time course of recovery, if at all. Conversely, if a short test wavelength is used, the rod system will be favored, and the cone-rod break occurs earlier in the time course of adaptation. If stimuli are small enough and centered at the foveola, then the normal dark adaptation curve is always monophasic, consisting only of the initial cone portion of the curve.[66]

One of the most popular devices for performing clinical dark adaptation manually was the Goldmann-Weekers Dark Adaptometer, which is still used today in some centers.[20; 53] This has largely been supplanted by automated techniques. For example, modifications of the 700 series of the Humphrey Visual Field Analyzer (HVFA) have been undertaken to enable the device to perform dark adaptometry.[47; 56; 90; 131; 132] Generally, an external illumination source is required to provide a "bleaching" light and an external computer controls the motor of the neutral density wheel in the optical path of the stimulus. Currently, there are commercially available devices for recording dark adaptation curves. One such dedicated device is the AdaptDx® (MacuLogix, Hummelstown, PA), launched initially in 2014.[54; 59; 60; 137] The device uses a short, intense period of light adaptation to cyan light at 505nm (default 0.8ms, estimated to be equivalent to an 83% rod bleach; see Table 1) to a 4° x 4° field. Sensitivity is subsequently determined for 2° cyan (505nm) circular stimuli. At around the same time, the MetroVision® (Paris, France) released a range of perimeters (MonCV series) with inbuilt dark adaptation capabilities. The MonCVOne CR allows the user to specify the adaptation duration, intensity (600cd.m^{-2} for 5 minutes on our device) and the test location post-bleach. The stimulus size is set at 1.7° (Goldmann size V); both white and narrow-band stimuli are available (410nm, 480nm, 560nm, 640nm) and testing with one or all stimulus colors is possible. The default stimulus presentation time is 500 ms. Additionally, electrophysiology systems are currently

available which have dark adaptation protocols, including those from Diagnosys LLC (Cambridge, UK), Roland consult (Berlin, Germany) and LKC technologies (Gaithersburg, MD, USA).

There have also been a number of studies which have tracked the recovery of human cone and rod system sensitivity during dark adaptation electrophysiologically. The appearance of a rod-cone break in ERG recordings was shown over 60 years ago,[5] and in the last two decades or so, a number of protocols have been used to probe recovery in rods[4; 26; 27; 41; 135] and cones,[21; 22; 68; 84; 85] with direct inferences made regarding the kinetics of rod and cone photopigment regeneration through comparisons with reflection densitometry and psychophysics.

b. Perimetric approaches

Compared to the visual field measured under photopic conditions clinically (usually 10 $cd.m^{-2}$ in clinical perimetry)[125] the normal visual field at absolute threshold is comparatively flat. Its shape varies with stimulus wavelength: there is a central depression at the point of fixation corresponding to the rod-free zone for short-wavelength targets and a modest foveal peak for long wavelength targets (See Figure 5), reflecting transition from rod-mediated detection peripherally to M+L-cone mechanism mediated detection centrally.[125; 126] Spectral sensitivity assessment of the central 30° of the visual field with vector addition fitting of data suggests that for Goldmann size V (1.7°) targets under scotopic conditions, sensitivity can be adequately described by rod mechanism detection for targets <640nm in wavelength (see Table 1); however, at the point of fixation there is clear evidence of contribution from/isolation of the cones at wavelengths >560 nm (see Table 1).[125]

Isolation of the rod and cone mechanisms was a popular approach with manual perimeters, and was achieved by manipulation of the spectral quality of the stimulus and/or through manipulation of the background intensity. Scotopic perimetry was introduced in the mid-1980s as a means of separating cone from rod responses perimetrically.[62; 63] The impetus in doing so was the inability – at that time – of ERG techniques to track topographical changes in rod and cone function. The original method utilized a modified HVFA.[62; 63] A typical testing approach is to pharmacologically dilate the subject's pupil, dark adapt them and then probe sensitivity under scotopic conditions with a short wavelength (blue) and a long-wavelength (red) target. Testing is then repeated with a long wavelength target under photopic conditions (white background, typically 10$cd.m^{-2}$). Similar modifications of other perimeters for performing so-called "two color perimetry" have also been described[32; 43] and the approach has been used extensively to study visual function in retinal degeneration. [32; 43; 56; 62; 63; 92; 125] Until recently, such devices were not commercially available and were therefore primarily employed by clinical research laboratories. Currently, a few commercially available perimeters have

scotopic testing capabilities. The MonCVOne perimeter (MetroVision, Paris, France) is a projection-type perimeter that can test under scotopic conditions without a background (or with white and colored backgrounds[126] ranging from 0.032cd.m^{-2} to 320cd.m^{-2} in 0.5 log cd.m^{-2} steps) with a variety of test wavelengths mirroring those available for dark adaptation using Goldmann size V stimuli (see above). The default stimulus duration is 300ms (modifiable) and the dynamic range is 110dB for white stimuli and 70dB for chromatic stimuli. The Medmont Dark Adaptated Chromatic Perimeter® (Medmont International, Nunawading, Australia) was specially developed for scotopic testing.[18; 71; 134] It utilizes LEDs to produce 1.7° stimuli (Goldmann size V) with peak wavelengths at 505nm (cyan) and 625 nm (red) and the default stimulus presentation time is 200ms. Like the MonCVOne, it benefits from a wide dynamic range (75dB). The key features of commercially available devices for dark adaptation and scotopic perimetry are outlined in Table 2.

c. Microperimetric approaches

Microperimetric methods combine funduscopic techniques with clinical perimetry and directly correlate a retinal locus to function. The majority of approaches employ, by default, mesopic background levels.[125] This has the advantage of exploiting the limited dynamic range of these devices (when compared to the perimeters described above). Currently available devices present perimetric stimuli in Maxwellian view.[51] This has the advantage of negating variances due to individual differences in pupil size (unless the pupil of the eye is smaller in effective diameter than the entrance pupil of the device), an important advantage when testing under conditions of absolute threshold (see above).[126] Both the Nidek MP1® (Nidek Inc., Aichi, Japan) perimeter and the MAIA® (CenterVue Srl, Padova, Italy) perimeters now offer modifications for performing scotopic microperimetry.[130] The Nidek MP1-S (and now the MP3-S) provides testing with a Goldmann size V stimuli target. The disadvantage of the device is its limited dynamic range (20dB in its original form) which can be extended by introducing neutral density filters (by up to 2.0 log units/20dB). The S-MAIA device utilizes both red (627nm) and cyan (505nm) Goldmann size III stimuli (See Table 3).

d. Full-field stimulus testing

There can be distinct drawbacks in the perimetric assessment of patients with retinal disease under photopic conditions. These include difficulties with fixation owing to central field loss or nystagmus and unnecessary and lengthy assessments that are disheartening for patients. The full-field stimulus testing (FST) approach was developed specifically for these reasons.[106] FST is in some respects the psychophysical equivalent of the full-field electroretinogram. Early reports of this approach employed a perimeter-based (HVFA, Humphrey Allergan, San Leandro, California) Ganzfeld bowl with hardware modifications,[104] and were soon-after followed by software modifications to an ERG

Ganzfeld bowl (Espion ColorDome®, Diagnosys, Lowell MA, USA) which extended the dynamic range by 2 log units, thus permitting the assessment of patients with profound reductions in sensitivity.[105] A commercially available system was subsequently included with the Diagnosys Espion system.[70]

The original incarnation of FST utilized the standard staircasing protocol of the HVFA, similar to those previously described.[104] The current Espion FST testing protocol generates a frequency of seeing curve. Sensitivity is calculated as the stimulus intensity corresponding to a 50% accuracy of target detection, based upon the fitted sigmoidal frequency of seeing curve (see Figure 6). It offers various stimulus options in terms of stimulus color, including white, blue (465nm) or red (637nm). The stimulus presentation time is 4ms and its intensity can be varied over a 100dB range. As noted in Table 1, an FST protocol is also available on the MonCVOne CR for white, red (647nm or 655nm) and blue (455nm or 500nm) stimuli.

One early supposition was that sensitivities measured by FST would primarily reflect the sensitivity of the most sensitive retinal areas.[89; 104] However, studies comparing full-field scotopic perimetric techniques to FST suggest that the latter can be best predicted in light of the whole visual field results, rather than simply the most sensitive locus.[71] This is to be anticipated, even without invoking means of spatial summation as traditionally conceived (e.g. if we assume instead probability summation of stimulated non-summating retinal areas). FST protocols demonstrated the efficacy of sub-retinal gene-replacement therapy in Leber congenital amaurosis 2 in pivotal clinical trials.[111] Furthermore, it forms an essential component of postregulatory approval monitoring of patient outcomes.[38]

6. INTERPRETATION OF COMPLEX SCENES/PRACTICAL TASKS NEAR ABSOLUTE THRESHOLD

a. Subjective assessment of complex visual scenes

Detailed work on the subjective experience of research participants under scotopic conditions was conducted in the first half of the 20th century. For example, Craik and Vernon explored the perception of everyday objects (e.g. stylized clock faces) and more complex scenes under scotopic conditions and related this to threshold sensitivity.[35] The selection of military personnel with superior scotopic capabilities was an issue for both the "allies" and their adversaries in WWII.[30; 31; 96; 97] Consequently, research into this aspect of vision was conducted in earnest during the war and published subsequently. Key aspects of British efforts appear in an MRC report from 1957 by Pirenne and coworkers.[97] It is relevant today because it anticipates modern "simulated real-life" tasks discussed below that similarly seek to link performance at a complex task to performance at standard/clinical tasks, e.g. scotopic acuity and threshold sensitivity. These workers envisaged that

their scotopic vision test would distinguish those normal subjects with a high degree of "perceptual efficiency" under scotopic conditions, who might, for example, be specially selected for night-time duties. Their test has also been used to explore scotopic vision in congenital achromatopsia/rod monochromacy.[122] Pirenne and colleagues' test requires not only that subjects have an adequately high sensitivity, but that they can interpret correctly what they see under scotopic conditions. In the test, subjects were seated on a chair in a dark room and viewed (binocularly) a photographic copy of the Hogarth engraving entitled *Hudibras beats Sidrophel, and his man, Whacum* (see Figure 7) at a distance of 90 cm. The picture was illuminated with a dim light (such that the luminance of the tablecloth in the picture was estimated to be 0.00048 scotopic cd/m^2 in its modern recapitulation).[122] Subjects were required to describe the scene after being given specific instructions which do not vary and their reports are subsequently scored using a standard, if Byzantine, method. To what extent does absolute sensitivity dictate performance in the interpretation of complex scenes? Interestingly, the findings of both Pirenne and colleagues' original experiments[97] and subsequent experiments in Daltonians and achromats[122] suggest a significant correlation between the absolute threshold measured with standard psychophysical techniques and performance at this test.[122] The former finding led Pirenne and colleagues[97] to conclude that military personnel could be selected for night time duties using tests of absolute threshold.

The introduction of new approaches to treating inherited retinal diseases (IRDs) has driven the development of analogous tests of visual function, which in this case seek to replicate activities of daily living, rather than unusual scenes (see below). More simple tests involve the identification of everyday objects in patients with low vision and resemble in some respects the tests utilized by Craik and Vernon.[35] Such tests have been used to explore functional vision in patients following implementation of electronic retinal prostheses[45] and more recently following optogenetic gene therapy (assessed with concurrent electroencephalography, EEG).[113]

b. Simulation of navigation tasks

i. Multi-luminance Mobility Testing

The impetus for the development of the multi-luminance mobility test (MLMT) was the recognition that one of the key activities of daily living negatively impacted by IRDs was mobility/navigation. Furthermore, it was envisaged that one of the functional benefits of new therapies (such as gene replacement therapy) might be improvements in mobility. The test itself was developed to assess efficacy in phase 1-3 trials of *AAV.RPE65*/voretigene neparvovec gene therapy for Leber congenital amaurosis 2 (LCA2)[112] and assessment of its construct and content validity was performed independently in a non-interventional study.[33]

582

583 In this task, subjects must follow arrows marked within an obstacle course measuring 1.5m by 3m
584 enclosure.[33] Obstacles may be placed in the pathway of the subject, or adjacent to the path. In
585 addition to the requirement to identify the arrows within the course, subjects are required to navigate
586 raised stairs and a door. As with the "Hudibras" test described above, scoring of the test is via
587 assessment by two to three masked observers to derive a total number of errors, from which an
588 overall score is derived, with a pre-determined cut-off for passing.[33] Additionally, the time to
589 completion is recorded, with deviations from the course added as time penalties. As its name
590 obliquely implies, the test is performed at multiple pre-specific illuminance (rather than luminance)
591 levels of 1, 4, 10, 50, 100, 150, 200, 250 and 400 lux (though 100 and 150, together with 200 and
592 250 were combined in analysis).[33; 112] The change in minimum illuminance required to pass the MLMT
593 and changes in FST following treatment with AAV.RPE65/voretigene neparvovec have been shown to
594 demonstrate a statistically significant correlation (Pearson-R = 0.71).[112] Similar paradigms were
595 developed in parallel to assess the efficacy of a competing gene replacement strategy for LCA2.[10]
596 The MLMT itself was a key functional outcome measure in the pivotal trial of voretigene
597 neparvovec,[111] helping demonstrate a meaningful improvement in visual function, rather than simply
598 an improvement in an abstracted clinical task.
599

600 *ii. Streetlab platforms (Institut de la Vision)*

601 Investigators at the Institut de la Vision, Paris, developed a low vision rehabilitation suite over the
602 period of a decade[114] termed the "Streetlab". This is comprised of 3 different simulated
603 environments: an artificial street (also, somewhat confusingly, termed Streetlab), a stylized apartment
604 (Homelab) and a driving simulator. The Streetlab artificial streetscape aims to recreate a street
605 environment and is an enclosure measuring 9m x 7m and is 5.5m in height. It is illuminated evenly by
606 a set of luminaires that can provide constant light levels ranging from 0 to 2,000 lux and which can
607 be varied in correlated color temperature (2,700 to 6,500K).[114] A 3D sound system is also included,
608 as is the facility for objective measurement via integrated image capturing techniques. These include
609 an eye-tracker, a motion capture system, and inertial sensors which can record complex behavior
610 patterns that, at present, have been analyzed by predetermined metrics (e.g. preferred walking
611 speed), but which would lend themselves to artificial intelligence approaches, such as those applied to
612 animal behavioral data.[48] The combined platforms have been used to explore the relationship
613 between clinical tests of visual function (e.g. visual field) and performance at simulated activities of
614 daily living in patients with glaucoma,[82] and adaptations in gaze/eye movements in patients with
615 visual field loss secondary to rod-cone dystrophy/retinitis pigmentosa.[9]
616

iii. Virtual reality devices

Virtual reality (VR) based tests have recently been implemented, which seek to extract the most important aspects of the simulated tasks and courses. Aleman and coworkers describe a VR test based loosely on the principles of the MLMT described above.[3] In this task, the subject navigates a similar VR course in which arrows (red instead of black, and adjusted in luminance to ensure that they are just visible to the subject) mark the direction to be taken. A head tracker incorporated into the goggles and limb (hand/ankle) trackers monitor the patient's movements. In the practice phase, objects can be highlighted sequentially to facilitate familiarization with the task/to avoid collisions. Unlike the MLMT, there is no mechanical or auditory feedback. The luminance of the elements within the VR display can be varied systematically (between $<0.2 cd.m^{-2}$ and a maximum of $144 cd.m^{-2}$), and the virtual test area encompasses a total of 2mx3m. Unlike the MLMT described above, the software automatically measures the speed with which subjects perform the course and records errors of judgement with respect to the path and obstacles. A pilot study involving 4 patients with LCA2 and 6 control subjects suggests that this may be a promising approach for future studies.[3]

Knopf et al.[72] have developed a virtual reality obstacle course incorporating real world experiences such as walking along a crowded foot path or across a virtual carpark that can offer a safe, affordable, and standardized orientation and mobility assessment tool that provides objective outcome measures not previously achieved by physical courses.

Conclusion

Our understanding of the physical and physiological basis of vision at absolute threshold, as well as the adaptation of the visual system to absolute threshold, is well-developed, though some questions remain. As we have seen, there are distinct advantages to assessing photoreceptor mechanisms at absolute threshold in patients with retinal disease because adaptation may act to mask so-called $d_{1/2}$ loss of sensitivity (i.e. loss of sensitivity from pathology at the level of the photoreceptors).[126]

The interest in determining the absolute threshold of vision clinically has seen a renaissance as the result of emerging treatments for retinal diseases, such as voretigene neparvovec (AAV.RPE65) for LCA2.[83; 112] ISCEV standard clinical electrophysiology has well defined suprathreshold testing strategies that facilitate diagnosis and are useful for early disease monitoring.[101] The prospect of novel therapies for retinal disease has necessitated the exploration for new biomarkers to measure functional outcomes.[49] Absolute threshold tests provide this capability, and clinicians now have access to a variety of commercially available tests for assessing increment thresholds under conditions of absolute threshold. A suggested guide to clinical application is provided in Table 4. Conventional perimeters can assess sensitivity over a wide range of background luminances, with a dynamic range

of ≥ 7 log units/70dB. Although it is now possible to explore absolute threshold using so-called fundus-guided techniques,[130] they suffer the disadvantage of offering a limited dynamic range (2log units/20dB) that can cause significant ceiling effects without the incorporation of additional neutral density filters in the optical pathway of the stimulus. In addition to selective perimetric techniques for probing absolute sensitivity, FST[64; 104; 105] is now readily available for assessing patients with poor fixation and/or eye movement disorders such as nystagmus. Additionally, newer tests such as the multi-"luminance" mobility test[33] and the Streetlab[114] can assess the minimum light levels required for subjects to perform tasks that seek to simulate activities of daily living.

Method of literature search

PubMed was used to search for articles: no limits were placed on date, or language, of publication. Search terms included "rod threshold", "cone threshold", "dark adaptation" and "absolute threshold". The search was expanded using the "related articles" function in PubMed. Secondary sources were identified from the articles identified in the primary search. In addition, personal archives of references were accessed.

Acknowledgements

Supported by the Foundation Fighting Blindness award CD-CL-0816-0710-SYD (MPS).

Competing interests

None.

CRediT author statement

Matthew Simunovic: Conceptualization, Writing – original draft, review and editing; **John Grigg:** Writing – review and editing; **Omar Mahroo:** Writing – review and editing

677 **References**

678 1. Adhikari P, Zele AJ, Feigl B: The Post-Illumination Pupil Response (PIPR). Invest Ophthalmol Vis Sci
679 56:3838-3849, 2015
680 2. Ahnelt PK: The photoreceptor mosaic. Eye (Lond) 12 (Pt 3b):531-540, 1998
681 3. Aleman TS, Miller AJ, Maguire KH, et al.: A Virtual Reality Orientation and Mobility Test for
682 Inherited Retinal Degenerations: Testing a Proof-of-Concept After Gene Therapy. Clin Ophthalmol
683 15:939-952, 2021
684 4. Alim-Marvasti A, Bi W, Mahroo OA, et al.: Transient Smartphone "Blindness". N Engl J Med
685 374:2502-2504, 2016
686 5. Alpern M, Faris JJ: Note on the electrical response of the human eye during dark adaptation. J Opt
687 Soc Am 44:74-79, 1954
688 6. Alpern M, Rushton WA, Torii S: The attenuation of rod signals by bleachings. J Physiol 207:449-
689 461, 1970
690 7. Alpern M, Pugh EN, Jr.: The density and photosensitivity of human rhodopsin in the living retina. J
691 Physiol 237:341-370, 1974
692 8. Athanasiou D, Aguila M, Bellingham J, et al.: The molecular and cellular basis of rhodopsin retinitis
693 pigmentosa reveals potential strategies for therapy. Prog Retin Eye Res 62:1-23, 2018
694 9. Authie CN, Berthoz A, Sahel JA, Safran AB: Adaptive Gaze Strategies for Locomotion with
695 Constricted Visual Field. Front Hum Neurosci 11:387, 2017
696 10. Bainbridge JWB, Smith AJ, Barker SS, et al.: Effect of gene therapy on visual function in Leber's
697 congenital amaurosis. N. Engl. J. Med. 358:2231-2239, 2008
698 11. Barlow HB: Retinal noise and absolute threshold. J Opt Soc Am 46:634-639, 1956
699 12. Barlow HB: Purkinje shift and retinal noise. Nature 179:255-256, 1957
700 13. Barlow HB, Andrews DP: The site at which rhodopsin bleaching raises the scotopic threshold. Vision
701 Res 13:903-908, 1973
702 14. Barlow HB: Retinal and central factors in human vision limited by noise, in Barlow HB, Fatt P (eds):
703 Vertebrate photorecpetion. New York, Academic Press, 1977
704 15. Baylor DA, Lamb TD, Yau KW: The membrane current of single rod outer segments. J Physiol
705 288:589-611, 1979
706 16. Baylor DA, Matthews G, Yau KW: Two components of electrical dark noise in toad retinal rod
707 outer segments. J Physiol 309:591-621, 1980
708 17. Baylor DA, Nunn BJ, Schnapf JL: The photocurrent, noise and spectral sensitivity of rods of the
709 monkey Macaca fascicularis. J Physiol 357:575-607, 1984

710 18. Bennett LD, Metz G, Klein M, et al.: Regional Variations and Intra-/Intersession Repeatability for
711 Scotopic Sensitivity in Normal Controls and Patients With Inherited Retinal Degenerations. Invest
712 Ophthalmol Vis Sci 60:1122-1131, 2019
713 19. Bergmanson JP, Townsend WD: The morphology of the cat tapetum lucidum. Am J Optom Physiol
714 Opt 57:138-144, 1980
715 20. Bijveld MM, van Genderen MM, Hoeben FP, et al.: Assessment of night vision problems in patients
716 with congenital stationary night blindness. PLoS One 8:e62927, 2013
717 21. Binns A, Margrain TH: Evaluation of retinal function using the Dynamic Focal Cone ERG.
718 Ophthalmic Physiol Opt 25:492-500, 2005
719 22. Binns AM, Margrain TH: Evaluating retinal function in age-related maculopathy with the ERG
720 photostress test. Invest Ophthalmol Vis Sci 48:2806-2813, 2007
721 23. Birch DG, Hood DC, Nusinowitz S, Pepperberg DR: Abnormal activation and inactivation
722 mechanisms of rod transduction in patients with autosomal dominant retinitis pigmentosa and the pro-
723 23-his mutation. Invest Ophthalmol Vis Sci 36:1603-1614, 1995
724 24. Brigell M, Jeffrey BG, Mahroo OA, Tzekov R: ISCEV extended protocol for derivation and
725 analysis of the strong flash rod-isolated ERG a-wave. Doc Ophthalmol 140:5-12, 2020
726 25. Brown TM, Tsujimura S, Allen AE, et al.: Melanopsin-based brightness discrimination in mice and
727 humans. Curr Biol 22:1134-1141, 2012
728 26. Cameron AM, Mahroo OA, Lamb TD: Dark adaptation of human rod bipolar cells measured from
729 the b-wave of the scotopic electroretinogram. J Physiol 575:507-526, 2006
730 27. Cameron AM, Miao L, Ruseckaite R, et al.: Dark adaptation recovery of human rod bipolar cell
731 response kinetics estimated from scotopic b-wave measurements. J Physiol 586:5419-5436, 2008
732 28. Campbell FW, Rushton WA: Measurement of the scotopic pigment in the living human eye. J
733 Physiol 130:131-147, 1955
734 29. Cao D, Nicandro N, Barrionuevo PA: A five-primary photostimulator suitable for studying
735 intrinsically photosensitive retinal ganglion cell functions in humans. J Vis 15:15 11 27, 2015
736 30. Chapanis A: The dark adaptation of the color anomalous. Fed Proc 5:16, 1946
737 31. Chapanis A: The Dark Adaptation of the Color Anomalous Measured with Lights of Different Hues.
738 J Gen Physiol 30:423-437, 1947
739 32. Chen C, Wu L, Wu D, et al.: The local cone and rod system function in early age-related macular
740 degeneration. Doc Ophthalmol 109:1-8, 2004
741 33. Chung DC, McCague S, Yu Z-F, et al.: Novel mobility test to assess functional vision in patients with
742 inherited retinal dystrophies. Clin. Experiment. Ophthalmol. 46:247-259, 2018
743 34. Cornwall MC, Fain GL: Bleached pigment activates transduction in isolated rods of the
744 salamander retina. J Physiol 480 (Pt 2):261-279, 1994

745 35. Craik K, Vernon M: Perception during dark adaptation. British Journal of Psychology 32:206-230,
746 1942
747 36. Curcio CA, Allen KA: Topography of ganglion cells in human retina. J Comp Neurol 300:5-25,
748 1990
749 37. Dartnall HJ, Bowmaker JK, Mollon JD: Human visual pigments: microspectrophotometric results
750 from the eyes of seven persons. Proc R Soc Lond B Biol Sci 220:115-130, 1983
751 38. Deutsche Ophthalmologische G, Berufsverband der Augenarzte Deutschlands e V, Retinologische
752 Gesellschaft e V: [Statement of the German Society of Ophthalmology (DOG), the German Retina
753 Society (RG) and the Professional Association of German Ophthalmologists (BVA) on the therapeutic
754 use of voretigene neparvovec-rzyl (Luxturna) in ophthalmology : Situation January 2019].
755 Ophthalmologe 116:524-533, 2019
756 39. Dey A, Zele AJ, Feigl B, Adhikari P: Threshold vision under full-field stimulation: Revisiting the
757 minimum number of quanta necessary to evoke a visual sensation. Vision Res 180:1-10, 2021
758 40. Dimitrov PN, Guymer RH, Zele AJ, et al.: Measuring rod and cone dynamics in age-related
759 maculopathy. Invest Ophthalmol Vis Sci 49:55-65, 2008
760 41. Dimopoulos IS, Tennant M, Johnson A, et al.: Subjects with unilateral neovascular AMD have
761 bilateral delays in rod-mediated phototransduction activation kinetics and in dark adaptation
762 recovery. Invest Ophthalmol Vis Sci 54:5186-5195, 2013
763 42. Dowling JE: Chemistry of visual adaptation in the rat. Nature 188:114-118, 1960
764 43. Drum B: Hybrid perimetry: a blend of static and kinetic techniques. Appl Opt 26:1415-1420,
765 1987
766 44. Dryja TP, Hahn LB, Reboul T, Arnaud B: Missense mutation in the gene encoding the alpha subunit
767 of rod transducin in the Nougaret form of congenital stationary night blindness. Nat Genet 13:358-
768 360, 1996
769 45. Edwards TL, Cottriall CL, Xue K, et al.: Assessment of the Electronic Retinal Implant Alpha AMS in
770 Restoring Vision to Blind Patients with End-Stage Retinitis Pigmentosa. Ophthalmology 125:432-443,
771 2018
772 46. Finkelstein D, Gouras P, Hoff M: Human electroretinogram near the absolute threshold of vision.
773 Invest Ophthalmol 7:214-218, 1968
774 47. Fitzke FW: Dark adaptation in retinal abnormalities. Br J Ophthalmol 78:426, 1994
775 48. Geuther BQ, Deats SP, Fox KJ, et al.: Robust mouse tracking in complex environments using neural
776 networks. Communications Biology 2:124, 2019
777 49. Grigg JR, Jamieson R, Chen F, et al.: Guidelines for the assessment and management of patients
778 with inherited retinal degenerations (IRD). Sydney, Australia, Royal Australian and New Zealand
779 College of Ophthalmologists, 2020

780 50. Guler AD, Ecker JL, Lall GS, et al.: Melanopsin cells are the principal conduits for rod-cone input
781 to non-image-forming vision. Nature 453:102-105, 2008
782 51. Han RC, Jolly JK, Xue K, MacLaren RE: Effects of pupil dilation on MAIA microperimetry. Clin Exp
783 Ophthalmol 45:489-495, 2017
784 52. Hecht S, Shlaer S, Pirenne MH: Energy, Quanta, and Vision. J Gen Physiol 25:819-840, 1942
785 53. Hess K, Gliem M, Birtel J, et al.: Impaired Dark Adaptation Associated with a Diseased Bruch
786 Membrane in Pseudoxanthoma Elasticum. Retina 40:1988-1995, 2020
787 54. Higgins BE, Taylor DJ, Binns AM, Crabb DP: Are Current Methods of Measuring Dark Adaptation
788 Effective in Detecting the Onset and Progression of Age-Related Macular Degeneration? A Systematic
789 Literature Review. Ophthalmol Ther 10:21-38, 2021
790 55. Holmes R, Victora M, Wang RF, Kwiat PG: Measuring temporal summation in visual detection with
791 a single-photon source. Vision Res 140:33-43, 2017
792 56. Holz FG, Jubb C, Fitzke FW, et al.: Dark adaptation and scotopic perimetry over 'peau d'orange'
793 in pseudoxanthoma elasticum. Br J Ophthalmol 78:79-80, 1994
794 57. Hood DC, Greenstein V: Models of the normal and abnormal rod system. Vision Res 30:51-68,
795 1990
796 58. Ingram NT, Sampath AP, Fain GL: Why are rods more sensitive than cones? J Physiol 594:5415-
797 5426, 2016
798 59. Jackson GR, Edwards JG: A short-duration dark adaptation protocol for assessment of age-
799 related maculopathy. J Ocul Biol Dis Infor 1:7-11, 2008
800 60. Jackson GR, Scott IU, Kim IK, et al.: Diagnostic sensitivity and specificity of dark adaptometry for
801 detection of age-related macular degeneration. Invest Ophthalmol Vis Sci 55:1427-1431, 2014
802 61. Jacobs GH, Neitz M, Neitz J: Mutations in S-cone pigment genes and the absence of colour vision
803 in two species of nocturnal primate. Proc Biol Sci 263:705-710, 1996
804 62. Jacobson SG, Voigt WJ, Parel JM, et al.: Automated light- and dark-adapted perimetry for
805 evaluating retinitis pigmentosa. Ophthalmology 93:1604-1611, 1986
806 63. Jacobson SG, Apathy PP, Parel JM: Rod and cone perimetry: computerized testing and analysis,
807 in Marshall DK (ed): Principles and practice of clinical electrophysiology of vision St. Louis, Mosby
808 Year Book, Inc., 1991
809 64. Jacobson SG, Aleman TS, Cideciyan AV, et al.: Defining the residual vision in leber congenital
810 amaurosis caused by RPE65 mutations. Invest Ophthalmol Vis Sci 50:2368-2375, 2009
811 65. Kalloniatis M, Harwerth RS: Differential Adaptation of Cone Mechanisms Explains the Preferential
812 Loss of Short-Wavelength Cone Sensitivity in Retinal Disease, in Drum B, Verriest G (eds): Colour
813 Vision Deficiencies IX, Vol. 52. Netherlands, Springer, 1989, pp. 353-364

66. Kalloniatis M, Luu C: Light and Dark Adaptation, in Kolb H, Fernandez E, Nelson R (eds): Webvision: The Organization of the Retina and Visual System. Salt Lake City (UT), 1995

67. Kay RF, Kirk EC: Osteological evidence for the evolution of activity pattern and visual acuity in primates. Am J Phys Anthropol 113:235-262, 2000

68. Kenkre JS, Moran NA, Lamb TD, Mahroo OA: Extremely rapid recovery of human cone circulating current at the extinction of bleaching exposures. J Physiol 567:95-112, 2005

69. Kirk EC: Comparative morphology of the eye in primates. Anat Rec A Discov Mol Cell Evol Biol 281:1095-1103, 2004

70. Klein M, Birch DG: Psychophysical assessment of low visual function in patients with retinal degenerative diseases (RDDs) with the Diagnosys full-field stimulus threshold (D-FST). Doc Ophthalmol 119:217-224, 2009

71. Klein M, Bennett LD, Kiser K, et al.: A Comparison of the Medmont Dark Adapted Chromatic Perimeter (DAC) with the Full-Field Stimulus Threshold (FST) in Subjects with Retinitis Pigmentosa (RP). Investigative Ophthalmology & Visual Science 57:631-631, 2016

72. Knopf NA, Boon M, Suaning GJ, et al.: Initial mobility behaviors of people with visual impairment in a virtual environment using a mixed methods design: 2017 IEEE Life Sciences Conference (LSC), 2017, pp. 153-156

73. Koenig D, Hofer H: The absolute threshold of cone vision. J Vis 11, 2011

74. Lamb TD: The involvement of rod photoreceptors in dark adaptation. Vision Res 21:1773-1782, 1981

75. Lamb TD: Sources of noise in photoreceptor transduction. J Opt Soc Am A 4:2295-2300, 1987

76. Lamb TD: Dark adaptation: a re-examination, in Hess R, Sharpe L, Nordby K (eds): Night Vision. Cambridge, Cambridge University Press, 1990, pp. 177-222

77. Lamb TD, Pugh EN, Jr.: Dark adaptation and the retinoid cycle of vision. Prog Retin Eye Res 23:307-380, 2004

78. Lamb TD, Pugh EN, Jr.: Phototransduction, dark adaptation, and rhodopsin regeneration the proctor lecture. Invest Ophthalmol Vis Sci 47:5137-5152, 2006

79. Lamb TD, Corless RM, Pananos AD: The kinetics of regeneration of rhodopsin under enzyme-limited availability of 11-cis retinoid. Vision Res 110:23-33, 2015

80. Lennie P, Fairchild MD: Ganglion cell pathways for rod vision. Vision Res 34:477-482, 1994

81. Lohse MJ, Maiellaro I, Calebiro D: Kinetics and mechanism of G protein-coupled receptor activation. Curr Opin Cell Biol 27:87-93, 2014

82. Lombardi M, Zenouda A, Azoulay-Sebban L, et al.: Correlation Between Visual Function and Performance of Simulated Daily Living Activities in Glaucomatous Patients. J Glaucoma 27:1017-1024, 2018

83. Maguire AM, Russell S, Wellman JA, et al.: Efficacy, Safety, and Durability of Voretigene Neparvovec-rzyl in RPE65 Mutation-Associated Inherited Retinal Dystrophy: Results of Phase 1 and 3 Trials. Ophthalmology 126:1273-1285, 2019

84. Mahroo OA, Lamb TD: Recovery of the human photopic electroretinogram after bleaching exposures: estimation of pigment regeneration kinetics. J Physiol 554:417-437, 2004

85. Mahroo OA, Lamb TD: Slowed recovery of human photopic ERG a-wave amplitude following intense bleaches: a slowing of cone pigment regeneration? Doc Ophthalmol 125:137-147, 2012

86. Makous W: Absolute sensitivity, in Hess R, Sharpe L, Nordby K (eds): Night Vision. Cambridge, Cambridge University Press, 1990, pp. 335-389

87. Masland RH: The neuronal organization of the retina. Neuron 76:266-280, 2012

88. Mata NL, Radu RA, Clemmons RC, Travis GH: Isomerization and oxidation of vitamin a in cone-dominant retinas: a novel pathway for visual-pigment regeneration in daylight. Neuron 36:69-80, 2002

89. Messias K, Jagle H, Saran R, et al.: Psychophysically determined full-field stimulus thresholds (FST) in retinitis pigmentosa: relationships with electroretinography and visual field outcomes. Doc Ophthalmol 127:123-129, 2013

90. Moore AT, Fitzke FW, Kemp CM, et al.: Abnormal dark adaptation kinetics in autosomal dominant sector retinitis pigmentosa due to rod opsin mutation. Br J Ophthalmol 76:465-469, 1992

91. Osorio D, Nilsson DE: Visual pigments: trading noise for fast recovery. Curr Biol 14:R1051-1053, 2004

92. Owsley C, Jackson GR, Cideciyan AV, et al.: Psychophysical evidence for rod vulnerability in age-related macular degeneration. Invest Ophthalmol Vis Sci 41:267-273, 2000

93. Pant M, Zele AJ, Feigl B, Adhikari P: Light adaptation characteristics of melanopsin. Vision Res 188:126-138, 2021

94. Paupoo AA, Mahroo OA, Friedburg C, Lamb TD: Human cone photoreceptor responses measured by the electroretinogram [correction of electoretinogram] a-wave during and after exposure to intense illumination. J Physiol 529 Pt 2:469-482, 2000

95. Pianta MJ, Kalloniatis M: Characterisation of dark adaptation in human cone pathways: an application of the equivalent background hypothesis. J Physiol 528:591-608, 2000

96. Pinson EA, Chapanis A: The relationship between measures of night vision and dark adaptation. Fed Proc 5:81, 1946

97. Pirenne MH, Marriott FHC, O'Doherty EF: Individual differences in night-vision efficiency. London, Medical Research Council, 1957

98. Pugh EN: Rushton's paradox: rod dark adaptation after flash photolysis. J Physiol 248:413-431, 1975

884 99. Pugh EN, Jr.: The discovery of the ability of rod photoreceptors to signal single photons. J Gen
885 Physiol 150:383-388, 2018
886 100. Reuter T: Fifty years of dark adaptation 1961-2011. Vision Res 51:2243-2262, 2011
887 101. Robson AG, Nilsson J, Li S, et al.: ISCEV guide to visual electrodiagnostic procedures. Doc
888 Ophthalmol 136:1-26, 2018
889 102. Robson JG, Troy JB: Nature of the maintained discharge of Q, X, and Y retinal ganglion cells of
890 the cat. J Opt Soc Am A 4:2301-2307, 1987
891 103. Robson JG, Saszik SM, Ahmed J, Frishman LJ: Rod and cone contributions to the a-wave of the
892 electroretinogram of the macaque. J Physiol 547:509-530, 2003
893 104. Roman AJ, Schwartz SB, Aleman TS, et al.: Quantifying rod photoreceptor-mediated vision in
894 retinal degenerations: dark-adapted thresholds as outcome measures. Exp Eye Res 80:259-272,
895 2005
896 105. Roman AJ, Cideciyan AV, Aleman TS, Jacobson SG: Full-field stimulus testing (FST) to quantify
897 visual perception in severely blind candidates for treatment trials. Physiological Measurement
898 28:N51-N56, 2007
899 106. Roman AJ, Cideciyan AV, Wu V, et al.: Full-field stimulus testing: Role in the clinic and as an
900 outcome measure in clinical trials of severe childhood retinal disease. Prog Retin Eye Res:101000,
901 2021
902 107. Rushton WA: Rhodopsin measurement and dark-adaptation in a subject deficient in cone vision. J
903 Physiol 156:193-205, 1961
904 108. Rushton WA: Dark-adaptation and the regeneration of rhodopsin. J Physiol 156:166-178, 1961
905 109. Rushton WA, Westheimer G: The effect upon the rod threshold of bleaching neighbouring rods. J
906 Physiol 164:318-329, 1962
907 110. Rushton WA: Bleached rhodopson and visual adaptation. J Physiol 181:645-655, 1965
908 111. Russell S, Bennett J, Wellman JA, et al.: Efficacy and safety of voretigene neparvovec (AAV2-
909 hRPE65v2) in patients with RPE65-mediated inherited retinal dystrophy: a randomised, controlled,
910 open-label, phase 3 trial. Lancet 390:849-860, 2017
911 112. Russell S, Bennett J, Wellman JA, et al.: Efficacy and safety of voretigene neparvovec (AAV2-
912 hRPE65v2) in patients with RPE65-mediated inherited retinal dystrophy: a randomised, controlled,
913 open-label, phase 3 trial. Lancet 390:849-860, 2017
914 113. Sahel JA, Boulanger-Scemama E, Pagot C, et al.: Partial recovery of visual function in a blind
915 patient after optogenetic therapy. Nat Med 27:1223-1229, 2021
916 114. Sahel JA, Grieve K, Pagot C, et al.: Assessing photoreceptor status in retinal dystrophies: from
917 high resolution imaging to functional vision. Am J Ophthalmol, 2021
918 115. Schulze M: Zur anatomie und physiologie der retina. Bonn, Verlag von Max Cohen & Sohn, 1866

116. Seiple W, Greenstein VC, Holopigian K, et al.: A method for comparing psychophysical and multifocal electroretinographic increment thresholds. Vision Res 42:257-269, 2002

117. Seiple WH, Holopigian K, Greenstein VC, Hood DC: Sites of cone system sensitivity loss in retinitis pigmentosa. Invest Ophthalmol Vis Sci 34:2638-2645, 1993

118. Sharpe L: Dark adaptation: a re-examination, in Hess R, Sharpe L, Nordby K (eds): Night Vision. Cambridge, Cambridge University Press, 1990, pp. 177-222

119. Sharpe LT, Stockman A, Fach CC, Markstahler U: Temporal and spatial summation in the human rod visual system. J Physiol 463:325-348, 1993

120. Sieving PA, Frishman LJ, Steinberg RH: Scotopic threshold response of proximal retina in cat. J Neurophysiol 56:1049-1061, 1986

121. Sieving PA, Nino C: Scotopic threshold response (STR) of the human electroretinogram. Invest Ophthalmol Vis Sci 29:1608-1614, 1988

122. Simunovic MP, Regan BC, Mollon JD: Is color vision deficiency an advantage under scotopic conditions? Invest Ophthalmol Vis Sci 42:3357-3364, 2001

123. Simunovic MP: On seeing yellow: the case for, and against, short-wavelength light-absorbing intraocular lenses. Arch Ophthalmol 130:919-926, 2012

124. Simunovic MP: Acquired color vision deficiency. Surv Ophthalmol 61:132-155, 2016

125. Simunovic MP, Moore AT, MacLaren RE: Selective Automated Perimetry Under Photopic, Mesopic, and Scotopic Conditions: Detection Mechanisms and Testing Strategies. Transl Vis Sci Technol 5:10, 2016

126. Simunovic MP, Hess K, Avery N, Mammo Z: Threshold versus intensity functions in two-colour automated perimetry. Ophthalmic Physiol Opt 41:157-164, 2021

127. Solomon SG, Lennie P: The machinery of colour vision. Nat Rev Neurosci 8:276-286, 2007

128. Sonoda T, Lee SK: A Novel Role for the Visual Retinoid Cycle in Melanopsin Chromophore Regeneration. J Neurosci 36:9016-9018, 2016

129. Sonoda T, Schmidt TM: Re-evaluating the Role of Intrinsically Photosensitive Retinal Ganglion Cells: New Roles in Image-Forming Functions. Integr Comp Biol 56:834-841, 2016

130. Steinberg JS, Sassmannshausen M, Pfau M, et al.: Evaluation of Two Systems for Fundus-Controlled Scotopic and Mesopic Perimetry in Eye with Age-Related Macular Degeneration. Transl Vis Sci Technol 6:7, 2017

131. Steinmetz RL, Polkinghorne PC, Fitzke FW, et al.: Abnormal dark adaptation and rhodopsin kinetics in Sorsby's fundus dystrophy. Invest Ophthalmol Vis Sci 33:1633-1636, 1992

132. Steinmetz RL, Haimovici R, Jubb C, et al.: Symptomatic abnormalities of dark adaptation in patients with age-related Bruch's membrane change. Br J Ophthalmol 77:549-554, 1993

133. Stiles WS: The directional sensitivity of the retina and the spectral sensitivities of the rods and cones. Proc. R. Soc. Lond. B 127:64–105, 1939
134. Tan RS, Guymer RH, Luu CD: Repeatability of Retinal Sensitivity Measurements Using a Medmont Dark-Adapted Chromatic Perimeter in Healthy and Age-Related Macular Degeneration Cases. Transl Vis Sci Technol 7:3, 2018
135. Thomas MM, Lamb TD: Light adaptation and dark adaptation of human rod photoreceptors measured from the a-wave of the electroretinogram. J Physiol 518 (Pt 2):479-496, 1999
136. Tinsley JN, Molodtsov MI, Prevedel R, et al.: Direct detection of a single photon by humans. Nat Commun 7:12172, 2016
137. Tzaridis S, Hess K, Heeren TFC, et al.: Dark Adaptation in Macular Telangiectasia Type 2. Retina 40:2018-2025, 2020
138. Vaney DI: Neuronal coupling in rod-signal pathways of the retina. Invest Ophthalmol Vis Sci 38:267-273, 1997
139. Verdon WA, Schneck ME, Haegerstrom-Portnoy G: A comparison of three techniques to estimate the human dark-adapted cone electroretinogram. Vision Res 43:2089-2099, 2003
140. Volbrecht VJ, Shrago EE, Schefrin BE, Werner JS: Spatial summation in human cone mechanisms from 0 degrees to 20 degrees in the superior retina. J Opt Soc Am A Opt Image Sci Vis 17:641-650, 2000
141. Wassle H, Yamashita M, Greferath U, et al.: The rod bipolar cell of the mammalian retina. Vis Neurosci 7:99-112, 1991
142. Wassle H, Grunert U, Chun MH, Boycott BB: The rod pathway of the macaque monkey retina: identification of All-amacrine cells with antibodies against calretinin. J Comp Neurol 361:537-551, 1995
143. Wassle H: Parallel processing in the mammalian retina. Nat Rev Neurosci 5:747-757, 2004
144. Yau KW: Phototransduction mechanism in retinal rods and cones. The Friedenwald Lecture. Invest Ophthalmol Vis Sci 35:9-32, 1994
145. Yau KW, Hardie RC: Phototransduction motifs and variations. Cell 139:246-264, 2009
146. Zele AJ, Feigl B, Adhikari P, et al.: Melanopsin photoreception contributes to human visual detection, temporal and colour processing. Sci Rep 8:3842, 2018
147. Zhao X, Pack W, Khan NW, Wong KY: Prolonged Inner Retinal Photoreception Depends on the Visual Retinoid Cycle. J Neurosci 36:4209-4217, 2016

Figure 1. Peak sensitivities of the photopigments: rhodopsin (black), the S-cone photopigment (blue), the M-cone photopigment (green) and the L-cone photopigment (red) and melanopsin (cyan).[37]

Figure 2. Threshold versus intensity functions (log Troland) averaged for 10 normal subjects (rods – purple; M+L-cone mechanism green) and the anticipated effects of d_1 receptoral defects in cones (50% dotted line, 90% dot-dashed line) and rods loss (dotted purple line). Note that at absolute threshold, d_1 losses are evident, but may be masked during adaptation (i.e. where dotted and dot-dashed lines converge).

Figure 3. Photopigment regeneration according to exponential or rate-limited kinetics. *A*, Curves plot theoretical recovery of rod or cone photopigment in the dark following a range of bleaches assuming exponential recoveries with a single time constant. *B*, Curves assume that recovery is "rate-limited": initial recovery is linear and proceeds at a common rate following a range of bleaches. The latter formulation (the "MLP model") appears to provide a better fit to photopigment regeneration data from a range of studies (with different parameter values for rod and cone recovery respectively), although the rate appears to slow further following very intense bleaches. The x-axis values have been omitted as different values apply to cone and rod photopigment regeneration: following a near total bleach, recovery takes around 5 min for cones, but may take over 20 min for rod photopigment.

Figure 4. Dark adaptation curve for a normal subject measured with a 480nm stimulus. The first 10 minutes of the curve are generated by cone responses, which plateau before a first rapid (S_2) phase of rod recovery followed by a slower (S_3) rod phase.

Figure 5. The scotopic visual field measured with a modified Humphrey Visual Field Analyzer for a 440nm narrow-band Goldmann size V stimulus (left) demonstrating a central depression corresponding to the rod-free zone, and a 680nm stimulus (right) demonstrating a small peak, resulting from cone participation for centrally-presented long wavelength targets. X- and Y-axes represent Cartesian coordinates in the visual field and Z-axis represents sensitivity in dB.

Figure 6. Full-field stimulus threshold results using the Diagnosys Espion for a patient with Leber congenital amaurosis type 2 before (top row) and at 3 months (bottom row) following treatment

with *AAV.RPE65* (voretigene neparvovec). Results are presented as percentage probability of detection versus intensity and demonstrate a post treatment improvement of ~ 1.5 log units.

Figure *7*. *Hudibras beats Sidrophel, and his man, Whacum* by William Hogarth.

Table 1. Perimetric photoreceptor mechanism isolation by wavelength for Goldman size V targets presented under scotopic conditions. Difference in sensitivity (dB) calculated from vector curve fitting of mechanism templates. Positive values represent isolation of the rods from the M+L-cones and negative values *vice versa*.

Table 2. Key features of the AdaptDx, MonCVOne and Medmont DACP devices for assessing dark adaptation functions/scotopic thresholds.

Table 3. Comparison of the Nidek MP-1S and S-MAIA microperimeters.

Table 4. A suggested guide for specialized psychophysical testing of threshold based upon diagnosis, electrodiagnostics and conventional perimetry. ISCEV International society for clinical electrophysiological of vision, ffERG full-field electroretinogram, pERG pattern electroretinogram, FST full-field stimulus testing, MD mean deviation, LCA Leber congenital amaurosis, ARMD age-related macular degeneration.

1050 Figure 1

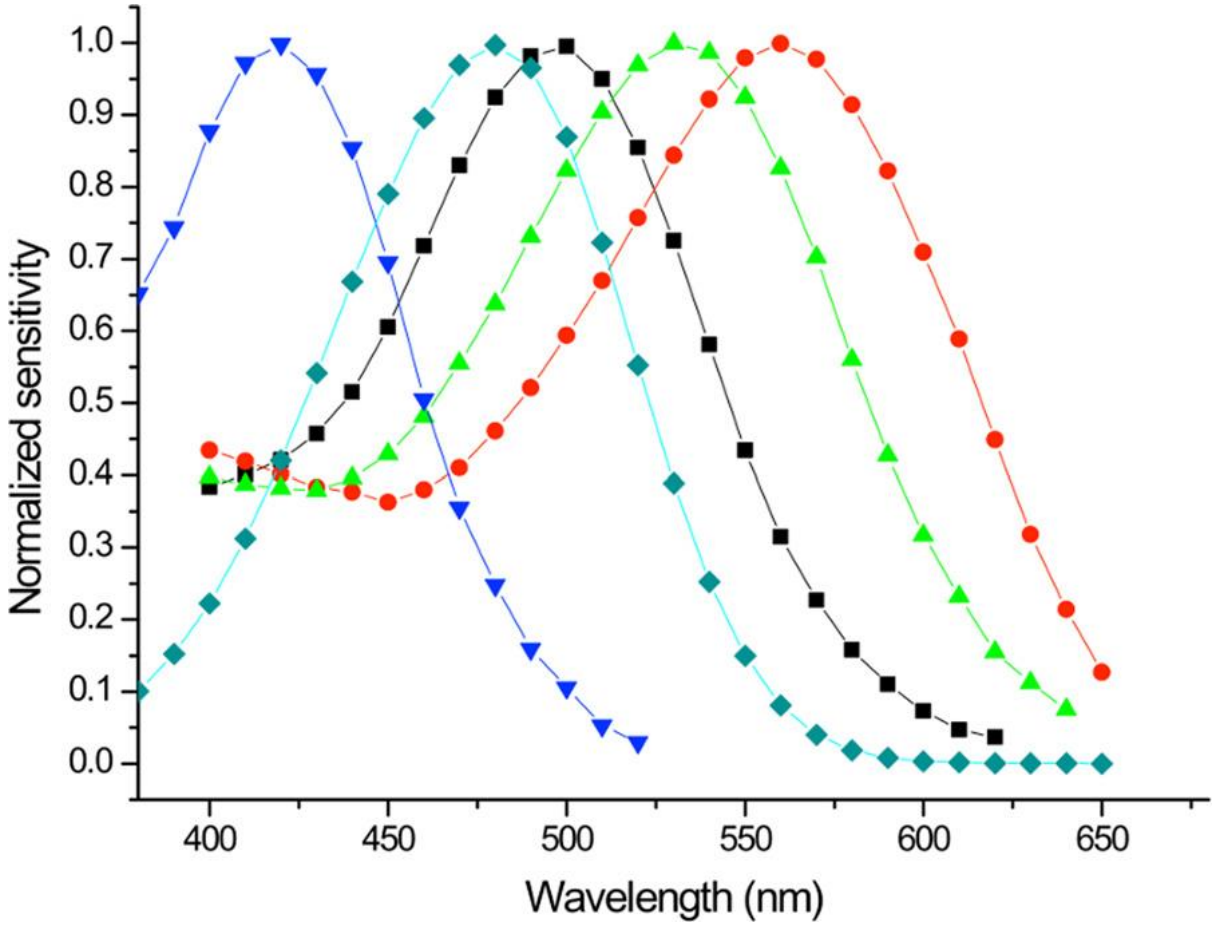

1051

1052

1053 Figure 2

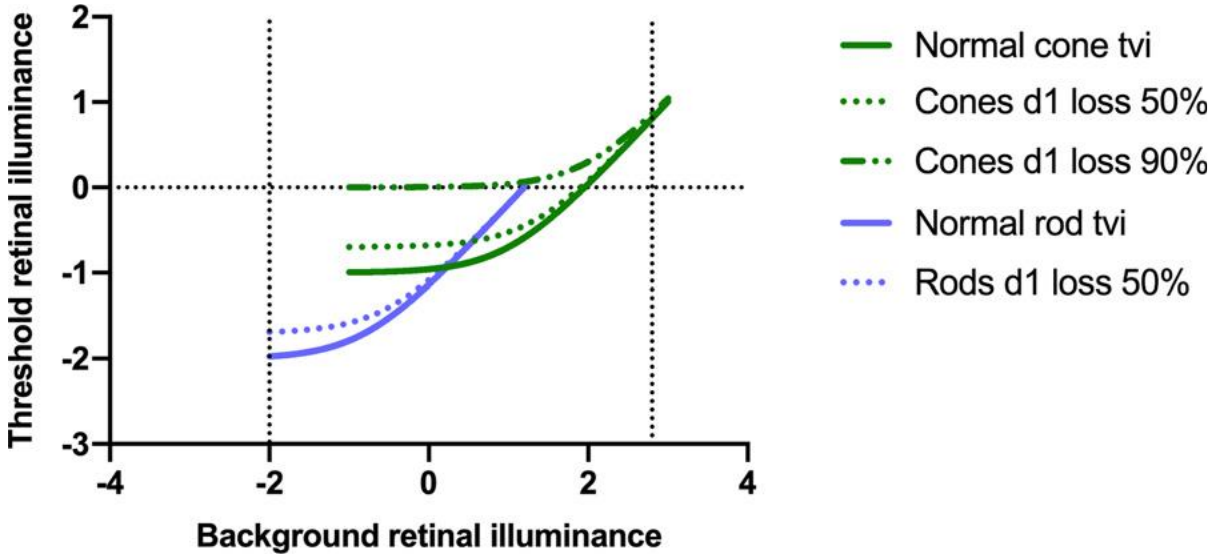

1054

1055

1056 Figure 3

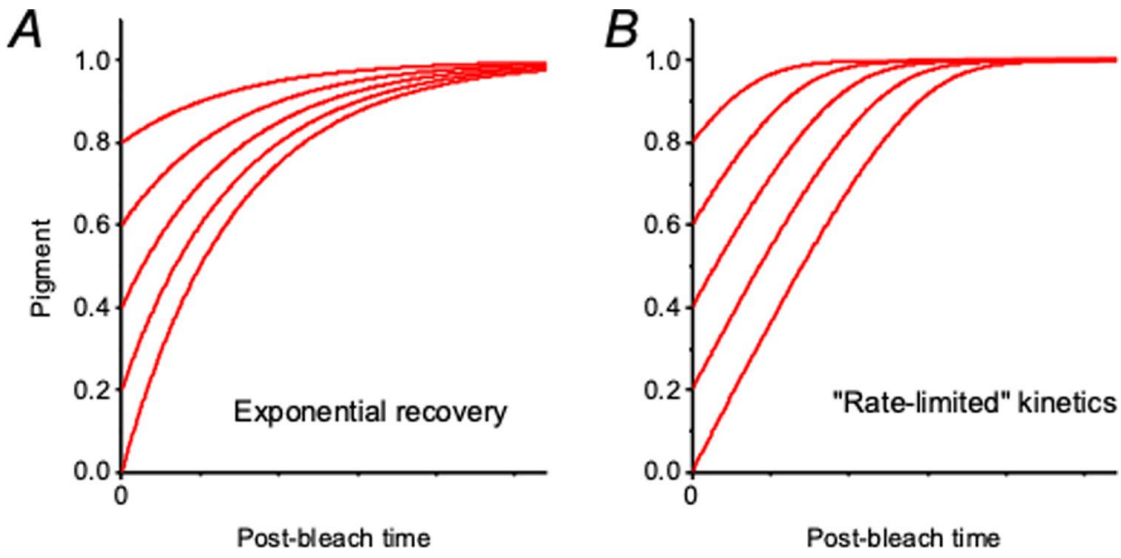

1057

1058

1059

Figure 4

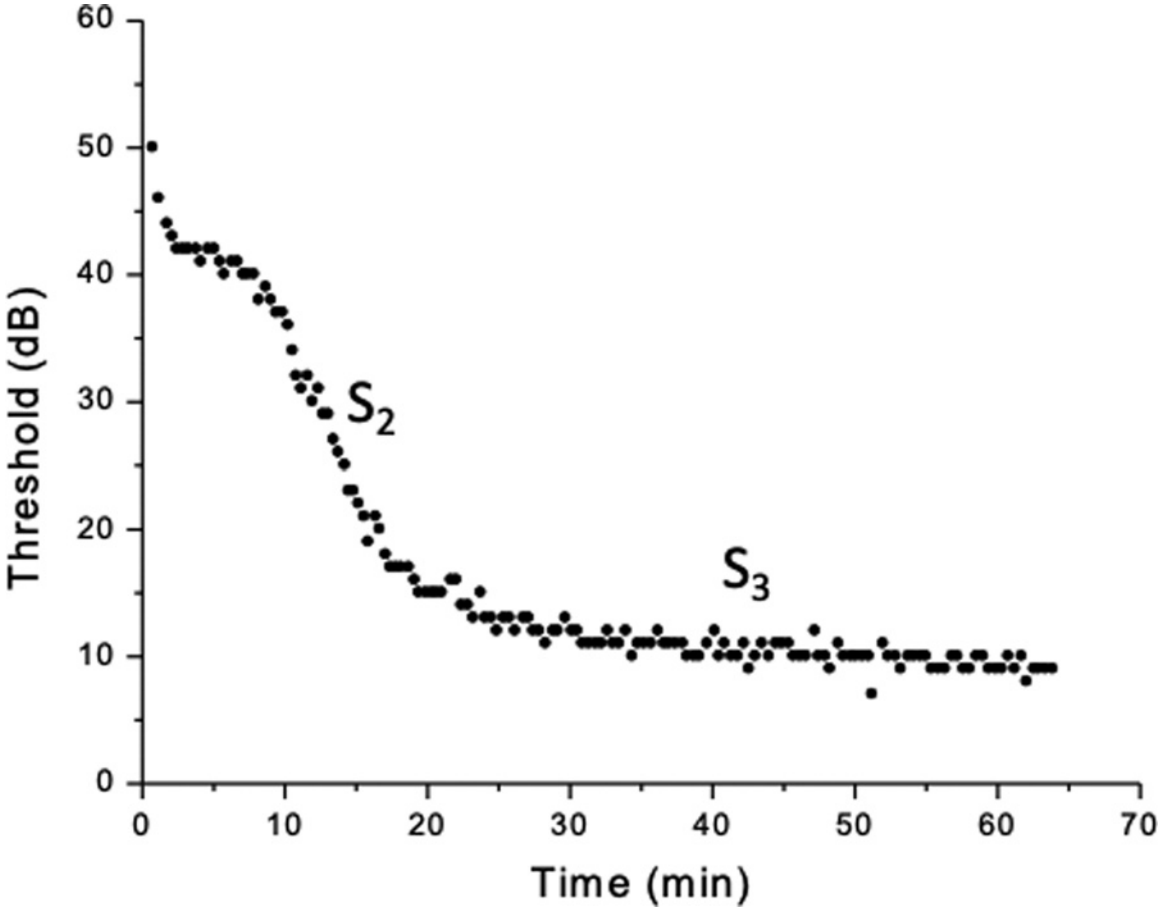

1064 Figure 5

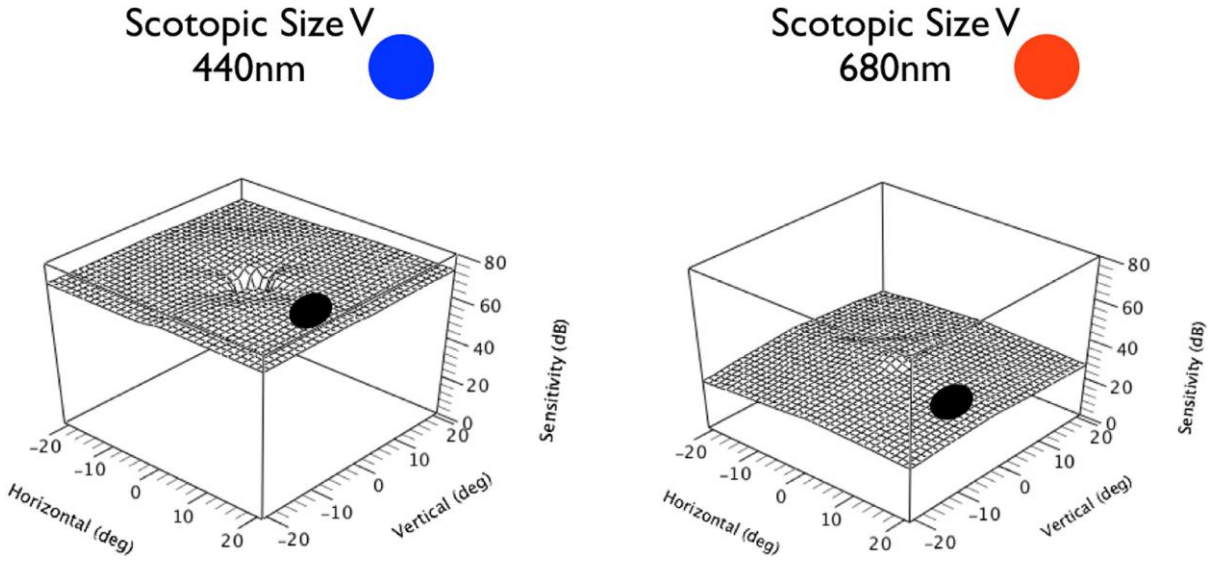

1065

1066

1067

1068 Figure 6

Pre-Rx
Right -1.740
Left -1.485

Post-Rx
Right -3.260
Left -3.285

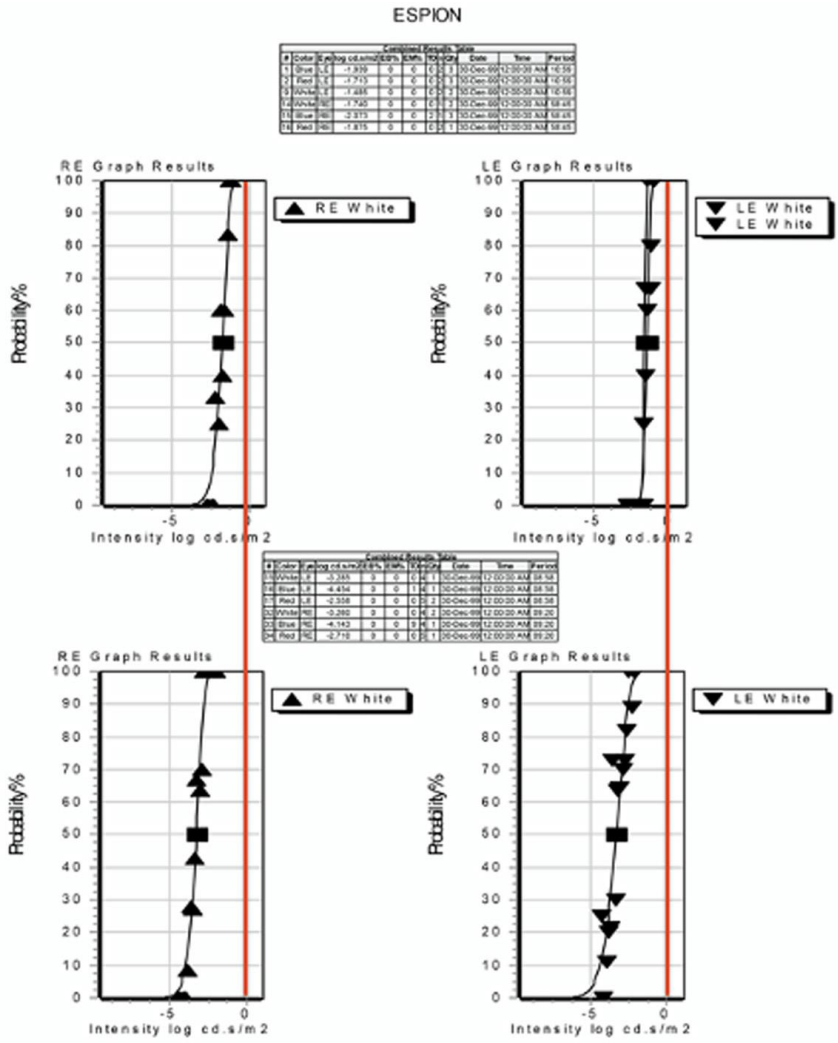

1069

1070

1071

Figure 7

1077 Table 1

Target wavelength	Isolation: Receptor Type	Magnitude of isolation		
		Periphery	[±3°, ±3°]	Fixation
410nm	Rods	≥ 36 dB	33 dB	16 dB
440nm	Rods	≥ 34 dB	31 dB	14 dB
480nm	Rods	≥ 31 dB	28 dB	11 dB
520nm	Rods	≥ 28dB	25 dB	8 dB
560nm	Rods	≥ 22 dB	19 dB	2dB
600nm	Rods (M+L-cones at fixation)	≥ 13 dB	10 dB	-7 dB (i.e. M+L-cones isolated)
640nm	Rods (M+L-cones at fixation)	≥ 3 dB	0 dB	-17 dB (i.e. M+L-cones isolated)
680nm	Rods (M+L-cones at fixation & [±3°, ±3°])	> 0 dB	-3 dB (i.e. M+L-cones isolated)	-20 dB (i.e. M+L-cones isolated)

1078

1079

1080

1081 Table 2

	AdaptDx	**MonCVOne-CR**	**Medmont-DACP**
Dark adaptation	Yes	Yes	Yes (no integral bleaching source)
Scotopic perimetry	No	Yes	Yes
Bleaching intensity & duration	18,000 scot.cd.m^{-2} for 0.8ms (default)/user-defined	600 cd.m^{-2} for 5 min (default)/user-defined	NA
Target size	2°	1.7° (GsV)	1.7° (GsV)
Target duration	200ms	500ms (DA) 300ms/user-defined (Scotopic perimetry)	200ms
Stimulus location	5, 8 or 12°	User-defined at any perimetric location	User-defined at any perimetric location
Target wavelength	505nm (Cyan)	White 420nm (Violet) 480nm (Blue) 560nm (Green) 640nm (Red)	505nm (Cyan) 625nm (Red)
Dynamic range	50dB	110dB (White) 70dB (Chromatic)	75dB
Full-field scotopic threshold testing?	No	Yes	No

1082

1083

1084

Table 3

Device	**MP-1S**	**S-MAIA**
Stimulus size	Goldmann V	Goldmann size III
Background luminance	0.0032cd.m^{-2}	<0.0001cd.m^{-2}
Stimulus duration	200ms	200ms
Threshold strategy	4-2dB	2-1dB
Dynamic range	20dB	20dB
Stimulus wavelength	NA (white)	Cyan 505nm Red 627nm
Maximum stimulus luminance	127cd.m^{-2}	0.08cd.m^{-2} (for both 505nm & 627nm)

1089 Table 4

1090

Suggested clinical indication for threshold psychophysical testing						
	ISCEV ffERG		ISCEV pERG		Threshold perimetry	Kinetic perimetry
Disorder / Symptom-sign	Normal	Undetectable	Normal	Abnormal	Severe Abnormal (MD >-12dB)	Abnormal
LCA	-	FST Mobility/navigation	-	-	-	FST Mobility/ navigation
Rod-cone dystrophy	-	FST Mobility/navigation	-	Microperimetry	Esterman binocular field	FST Mobility/ navigation
Unexplained Nyctalopia	Dark adaptometry		-	Microperimetry	-	-
Cone-Rod dystrophy	-	FST Mobility/navigation		Microperimetry	Microperimetry	-
Macular dystrophy	-	-		• Microperimetry • Dark adaptometry • Scotopic perimetry	Microperimetry	-
iARMD	-	-	• Dark adaptometry • Scotopic perimetry	• Microperimetry • Dark adaptometry • Scotopic perimetry	Microperimetry	-

1091